Available online at www.sciencedirect.com
SCIENCE DIRECT
Catalysis Today 116 (2006) 30–37
CATALYSIS TODAY
www.elsevier.com/locate/cattod

Kinetics of atom recombination at catalytic surfaces ruled by *hot atom* energy distributions

Ettore Molinari, Massimo Tomellini *

Dipartimento di Scienze e Tecnologie Chimiche, Università di Roma Tor Vergata, Via della Ricerca Scientifica, 00133 Roma, Italy

Available online 12 May 2006

Abstract

In the framework of the 'hot atom' reaction mechanism we report on the rate of adatom recombination at catalytic surfaces. The modeling deals with a flat surface where hot atoms are identified with the adatoms populating the excited states of the vibrational ladder of the adsorption potential well. The dynamics of the energy transfer between the adlayer and the solid, that is the exchange of vibrational quanta between the adatoms and the solid, has been explicitly taken into account in the master equations together with the adsorption and recombination processes. At steady state the analytical solution of the kinetics is found to be in good agreement with the numerical solutions for a four-levels system. It is shown that the recombination rate at steady state is strongly dependent upon the ratio between the probabilities (per unit time) of quantum dissipation to the solid and of adatom recombination. This ratio is a key quantity of the kinetic model since it rules a continuous transition towards higher rates which is ascribed to a progressive displacement of the vibrational state of the adlayer, from the equilibrium condition.
© 2006 Elsevier B.V. All rights reserved.

Keywords: Kinetics of adatom recombination; Adatom energy distribution; Non-equilibrium phenomena

1. Introduction

Modeling the reaction rates of exothermic processes at solid surfaces is a topic of great interest in heterogeneous catalysis also in connection to the dynamics of the energy relaxation of the adspecies at the catalyst surface. In fact, the energy released during the reaction may be either dissipated to the solid or used to excite both the desorbing molecules and the adspecies [1–3]. A fraction of the energy released during the reaction can therefore be employed to trigger reaction routes which are characterized by enhanced rates when compared to those expected under thermal equilibrium of the reacting adspecies. In the Langmuir Hinshelwood (LH) mechanism, for instance, diatom formation occurs by binary encounter of adatoms, which have thermally equilibrated with the surface, according to a second order reaction kinetics. On the other side, diatom formation can occur by direct abstraction of adatoms by gas atoms, that is according to the Eley–Rideal (ER) mechanism that implies a first order reaction kinetics [4]. A mechanism intermediate between the LH and ER calls for the *hot atom* (HA) concept, as firstly introduced in Ref. [5], concerning adatoms that are not thermally accommodated at the surface. The HA mechanism has been invoked to explain experimental data on the recombination and abstraction of hydrogen at metal surfaces [6–11] and the oxidation of carbon monoxide by atomic and molecular oxygen [12,13].

Modeling the HA mechanism requires the determination of the HA surface densities which, in the model case of flat surfaces, have been identified with the populations of the adatoms in the vibrational states of the adsorption potential well [10,13]. According to the associative model [14] the recombination rate is proportional to the product of the adatom populations provided the total energy of the couples is larger than twice the adsorption energy, that is the activation energy for desorption.

On the basis of these premises in this paper we present a multi-level HA kinetics for modeling the steady state rate of diatom formation. To this end a kinetic approach will be employed where the adsorption, the recombination and the dynamics of the vibrational relaxation of the adlayer are taken into account. One of the goals of this contribution is to investigate the role played by the dissipation of the vibrational energy of the adatoms in the recombination kinetics. The theoretical sections of the paper are mainly devoted to the

* Corresponding author. Tel.: +39 06 7259 4418; fax: +39 06 7259 4328.
E-mail address: tomellini@uniroma2.it (M. Tomellini).

0920-5861/$ – see front matter © 2006 Elsevier B.V. All rights reserved.
doi:10.1016/j.cattod.2006.04.001

evaluation of the steady state HA surface densities and recombination rates in case of single reaction channels, as well as to study the effect of multi-quantum energy transfer on the HA surface coverage. Besides, throughout the article the application of the main results of the theory to experimental data on adsorption stimulated desorption (ASD) will be also presented and discussed.

2. Results and discussion

2.1. Hot atom energy distribution functions

In this paper we deal with diatom recombination at a flat catalytic surface according to the process $2A_s \rightarrow A_2$, where A_s stands for the adspecies. In particular, on the basis of the aforementioned hypothesis adatoms populate the vibrational ladder of the 1D adsorption potential well, $V(z)$, z being the atom-surface distance along the normal to the surface. As far as the motion on the x–y plane is concerned, adatoms are free particles and the eigenvalue of the single particle Hamiltonian is given by $E_{p_x,p_y,v} = E_a + E_v + \varepsilon_{p_x,p_y}$, where ε_{p_x,p_y} is the kinetic energy for the motion on the x–y plane, E_a the adsorption energy and E_v is the vibrational energy, with v the vibrational quantum number. As anticipated in the introduction, one refers to adatoms populating the excited vibrational level as "hot". By means of the associative model [14] recombination and desorption of diatoms arise from adatoms in vibrational states v and v' according to $A_s(v) + A_s(v') \rightarrow A_2$, provided the constraint $2E_a + E_v + E_{v'} = E_{A_2} > 0$ is fulfilled. In this last inequality the kinetic energy term has been neglected when compared to the vibrational one. In other words, in the adsorption the atom momentum is conserved on the plane of the flat surface, the average value of the kinetic energy, $\langle \varepsilon_{p_x,p_y} \rangle$, is expected to be of the order of $k_B T \ll -E_a$, k_B being the Boltzmann constant and T the surface temperature. The rate of the single reaction channel is eventually given by $Z_{vv'}\sigma_v\sigma_{v'}$, where $Z_{vv'}$ is the rate constant and σ_v the surface coverage of adatoms in the v-th vibrational level. From this expression it stems that, to evaluate the reaction rate, the knowledge of the adatom vibrational populations is mandatory. To this end a rate equation approach is employed which accounts for the relevant processes that characterize the dynamics of the vibrational relaxation of the adlayer namely, the dissipation of vibrational quanta to the solid (VL process) and the exchange of vibrational quanta among the adatoms (VV process):

$$A_s(n) + L \underset{K^{(q)}_{-(n-q)}}{\overset{K^{(q)}_n}{\rightleftarrows}} A_s(n-q) + L^* \quad \text{(VL process)} \tag{1}$$

and

$$A_s(n) + A_s(m) \underset{P_{n-q,m+q\rightarrow n,m}}{\overset{P_{n,m\rightarrow n-q,m+q}}{\rightleftarrows}} A_s(n-q) + A_s(m+q)$$

$$\text{(VV process)} \tag{2}$$

where K and P are the first- and the second-order rate constants and the superscript q stands for the number of vibrational quanta exchanged in the scattering event. In Eq. (1) L and L^* stand for the substrate lattice and the excited lattice, respectively. Moreover, gas atoms enter the potential well from the upper bound level, $v^*(A \rightarrow A_s(v^*))$ and the vibrational energy is redistributed throughout the ladder by means of VV and VL processes.

By denoting with $I_{n,m}$ the net current of adatoms from level n to level $m < n$, due to the VV and VL scatterings, the master equations for the populations of adatoms read (see also Fig. 1):

$$\frac{d\sigma_n}{dt} = J(\sigma)\delta_{n,v^*} + \sum_{q=1}^{v^*-n} I_{n+q,n} - \sum_{q=1}^{n} I_{n,n-q} - \Phi_n \tag{3}$$

where Φ_n is the flux of adatoms that recombine from level n, $J(\sigma)$ the flux of atoms entering the adsorption well, $\sigma = \sum_n \sigma_n$ and $\delta_{i,j}$ is the Kronecker delta. The expression of $I_{n,n-q}$ is given by

$$I_{n,n-q} = (K_n^{(q)} + P_n^{r(q)})\sigma_n - (K_{-(n-q)}^{(q)} + P_{(n-q)}^{f(q)})\sigma_{n-q} \tag{4}$$

in which

$$P_n^{f(q)} = \sum_{s=q}^{v^*} P_{n,s\rightarrow n+q,s-q}\sigma_s \tag{5}$$

and

$$P_n^{r(q)} = \sum_{s=0}^{v^*-q} P_{n,s\rightarrow n-q,s+q}\sigma_s \tag{6}$$

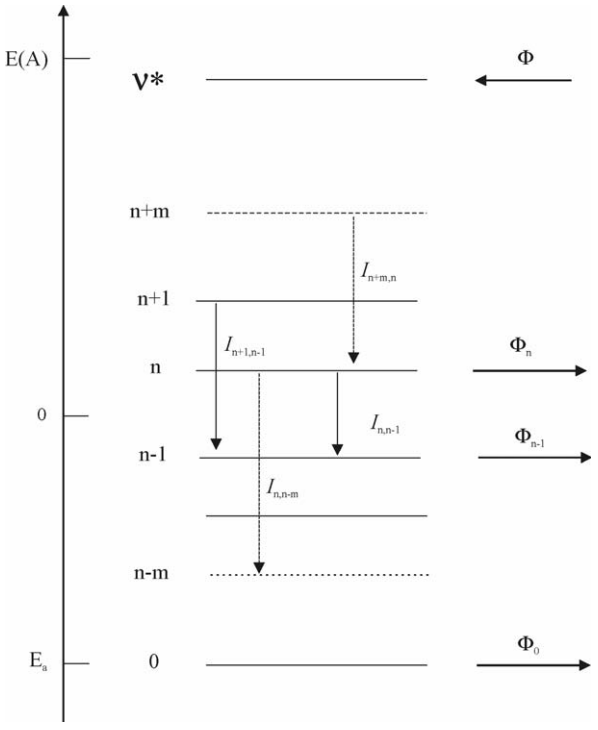

Fig. 1. Schematic representation of the vibrational ladder. Φ is the net flux of atoms incoming on the surface, Φ_n is the flux of adatoms leaving the n-th level because of the recombination process. The $I_{n,n-m}$ currents, between levels n and $n-m$, are linked to the VV and the VL quantum exchanges.

The recombination rate is modeled on the basis of the associative model through the relationship:

$$\Phi_n = \sigma_n \sum_{m=\mu(n)}^{v^*} Z_{mn}\sigma_m[1+\delta_{m,n}] \tag{7}$$

where the lower cut off in the sum stems from the inequality $2E_a + E_n + E_m = E_{A_2} > 0$ that has to be verified so that the reaction channel may be open. In Eq. (7) Z_{mn} denotes the rate constant for dimer formation.

The system equation (3) embodies the dynamics of HA relaxation in the potential well by considering also adsorption and recombination phenomena. The analytical solution of the kinetics, Eq. (3), is a very difficult task. Nevertheless, in some cases the steady state vibrational populations of the adatoms can be computed in closed form. Steady state is established at the end of the adsorption process when $J(\sigma) = \Phi = \sum_n \Phi_n$, Φ being the total rate of recombination. Since at steady state the coverage of adatoms is independent of time, the energy distribution of adatoms can be expressed as a function of the $I_{n,n-q}$ currents for an arbitrarily chosen value of q. As far as the rate constants of the reverse processes are concerned (Eqs. (1) and (2)), they are related to the ones of the forward reactions through the detailed balance: $(K^{(q)}_{-(n-q)}/K^{(q)}_n) = e^{-\beta(E_n - E_{n-q})}$ and $(P_{n,s\to n-q,s+q}/P_{n-q,s+q\to n,s}) = e^{-\beta(E_{n-q}+E_{s+q}-E_n-E_s)}$, where $\beta = (k_B T)^{-1}$, T being the temperature of the surface and k_B the Boltzmann constant. The computation simplifies in the case of a harmonic potential and for the rate constants $P_{n,s\to n-q,s+q}$ and $K^{(q)}_n$ independent of quantum numbers: $P_{n,s\to n-q,s+q} \equiv P^{(q)}_{VV}$ and $K^{(q)}_n \equiv K^{(q)}_{VL}$. As shown in Appendix A iteration of Eq. (4) at $q = 1$ leads to:

$$\sigma_n = \sigma_0 \gamma^{(1)^n} + \alpha^{(1)} \sum_{j=1}^{n} I_{j,j-1}\gamma^{(1)^{n-j}} \tag{8}$$

where $\alpha^{(1)} = [K^{(1)}_{VL} + P^{(1)}_{VV}(\sigma - \sigma_{v^*})]^{-1}$, $\gamma^{(1)} = \gamma^{(1)}_B(1+\xi^{(1)})$ with $\xi^{(1)} = (P^{(1)}_{VV}/\gamma^{(1)}_B K^{(1)}_{VL})\alpha^{(1)} \sum_{j=0}^{v^*-1} I_{j+1,j}$ and $\gamma^{(1)}_B = e^{-\beta E_{01}}$ with $E_{01} = E_1 - E_0$.

It is worth noting that Eq. (8) is quite general, in the sense that it can be applied for describing adatom populations in adsorption and chemisorption processes as well. In fact Eq. (8) can be employed to interpret experimental data on adsorption stimulated desorption (ASD). ASD defines the phenomenon revealed by isotope jump experiments carried out with CO on Rh, Pd, Ni and with H_2 on W [15 and references therein]. In these experiments the heavier isotope is preadsorbed up to a given σ. The surface is then exposed to the lighter isotope and the desorption kinetics of the heavier one is followed by mass spectrometer. The experimental results show that the rate of desorption is proportional to the adsorption rate. These rather puzzling findings can be explained on the basis of Eq. (8) by noting that the desorption rate is proportional to the population of the upper bound level σ_{v^*}. Furthermore, since we are dealing with an adsorption process, in Eq. (8) the equality $I_{j,j-1} = I$ holds, where I is the adsorption rate. As a consequence σ_{v^*} is proportional to the adsorption rate [15].

In case of adatom recombination Eq. (8) is evaluated under the following assumptions: (i) single quantum transfer ($q = 1$); (ii) adatom recombination occurs by either the reaction channel $A_s(p) + A_s(p) \to A_2$ (case A) or $A_s(0) + A_s(p) \to A_2$ (case B).

As far as the case A is concerned, we note that under steady state conditions, being $\dot{\sigma} = 0$, the mass balance implies $(I_{j,j-1})_{j>p} = \Phi$ and $(I_{j,j-1})_{j\le p} = 0$. For $\gamma^{(1)} \ll 1$ one obtains:

$$\sigma_{n\le p} = \sigma_0 \gamma^{(1)^n} \tag{9a}$$

$$\sigma_{n>p} = \sigma_0 \gamma^{(1)^n} + \frac{1}{[1 + P^{(1)}_{VV}(\sigma - \sigma_{v^*})/K^{(1)}_{VL}]} \frac{\Phi}{K^{(1)}_{VL}} \tag{9b}$$

with

$$\xi^{(1)} = \frac{1}{\gamma^{(1)}_B} \frac{P^{(1)}_{VV}/K^{(1)}_{VL}}{[1 + P^{(1)}_{VV}(\sigma - \sigma_{v^*})/K^{(1)}_{VL}]} \frac{(v^* - p)\Phi}{K^{(1)}_{VL}} \tag{9c}$$

where $\gamma^{(1)}_B = e^{-\beta E_{01}}$ and $\gamma^{(1)} = \gamma^{(1)}_B(1+\xi^{(1)})$ as defined in Eq. (8).

Eq. (9) shows that the steady state populations of HA are not thermal to an extent that depends upon the ratio between the recombination flux and the rate constant for energy dissipation to the solid ($K^{(1)}_{VL}$). As a matter of fact the equilibrium distribution, namely $\sigma_n = \sigma_0 \gamma^n_B$, is recovered for either $\Phi = 0$ or in the limit $K^{(1)}_{VV} \to \infty$. Thus, in exoergic catalytic reactions the surface density of HA is dictated by the competition between adsorption and quantum dissipation processes through the ratio $\Phi/K^{(1)}_{VL}$.

The validity of the distribution Eq. (9) has been tested through numerical integration of the system equation (3), in the case of four levels and for random adsorption of atoms, i.e. $J(\sigma) = J(1-\sigma)$, where J is the flux of gas atoms [16]. The numerical approach gives the entire kinetics of the adsorption-recombination process from $t = 0$, when the fractional surface coverage is zero, up to the steady state for $t \to \infty$. The comparison between the analytical and the numerical steady state solutions, $R_n = \sigma_n/\sigma_0$, is shown in Fig. 2. As appears the

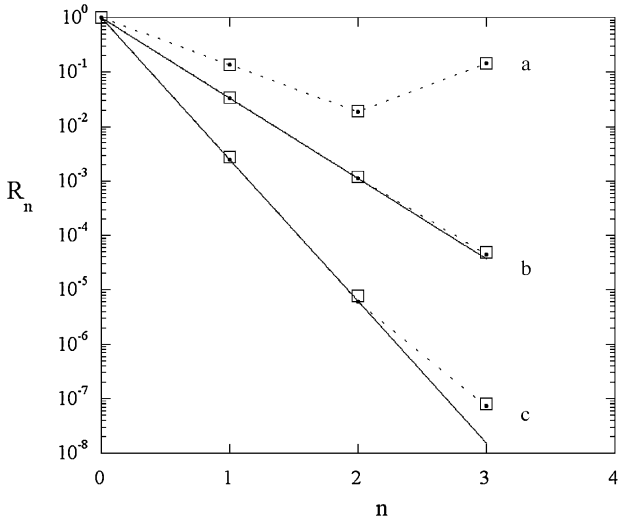

Fig. 2. Comparison between numerical (open symbols) and analytical (dots) solutions of the steady state HA populations in the case of four levels and for the reaction channel A: $R_n = \sigma_n/\sigma_0$. Parameter values are: $p = 2$, $Z_{pp} = 5 \times 10^{12}\ s^{-1}$, $P_{VV} = 10^{10}\ s^{-1}$ and (a) $K^{(1)}_{VL} = 7 \times 10^8\ s^{-1}$, $J = 10^7\ s^{-1}$, $\beta E_{01} = 3.4$; (b) $K^{(1)}_{VL} = 10^{12}\ s^{-1}$, $J = 10^7\ s^{-1}$, $\beta E_{01} = 3.4$; (c) $K^{(1)}_{VL} = 10^8\ s^{-1}$; $J = 10^5\ s^{-1}$, $\beta E_{01} = 6$. The Boltzmann distributions are also shown as full lines.

agreement between the two approaches is satisfactory. The numerical solutions can be also exploited in order to verify the quasi-steady state hypothesis that is often used for describing adsorption and recombination kinetics. To this end the kinetics of the adatom populations are computed by means of Eq. (9) for the instantaneous value of σ_0: $\sigma_0(t)$. The $\sigma_0(t)$ function is obtained by numerical integration of the master equation (Eq. (3)). The large difference between the characteristic times for adsorption and for VL (VV) relaxation, justifies the steady-state hypothesis. In Fig. 3 the kinetics of the adatom populations, as attained by numerical integration of rate equations, are compared with those computed on the ground of the steady state hypothesis (Eq. (9)). As expected the steady state approximation is verified the lower the $J/K_{\mathrm{VL}}^{(1)}$ value; in fact for $J/K_{\mathrm{VL}}^{(1)} = 10^{-5}$ (Fig. 3, panel b) the behavior of the $\sigma_n(t)/\sigma_0(t)$ ratio is in excellent agreement with the steady state solution. Fig. 3 (panels a, c) also shows that for larger values of the $J/K_{\mathrm{VL}}^{(1)}$ ratio the steady state approximation does not hold at $n = 1, 2$; clearly for long time, when the true steady state is approached, the numerical and the analytical curves coincide.

Let us now discuss the reaction channel B. Also in this case the mass balance allows one to estimate $I_{j,j-1}$ at steady state. Since we are dealing with diatom formation, via reaction pathway B, half of the recombination flux arises from adatoms in the level "p", the remaining from those in level "0". Therefore $(I_{j,j-1})_{j>p} = \Phi$, $(I_{j,j-1})_{j\le p} = \Phi/2$ and Eq. (8) yields ($\gamma^{(1)} \ll 1$):

$$\sigma_{n\le p} = \sigma_0 \gamma^{(1)^n} + \frac{1}{[1 + P_{\mathrm{VV}}^{(1)}(\sigma - \sigma_{v^*})/K_{\mathrm{VL}}^{(1)}]} \frac{\Phi}{2K_{\mathrm{VL}}^{(1)}} \tag{10a}$$

$$\sigma_{n>p} = \sigma_0 \gamma^{(1)^n} + \frac{1}{[1 + P_{\mathrm{VV}}^{(1)}(\sigma - \sigma_{v^*})/K_{\mathrm{VL}}^{(1)}]} \frac{\Phi}{K_{\mathrm{VL}}^{(1)}} \tag{10b}$$

where

$$\xi^{(1)} = \frac{1}{\gamma_{\mathrm{B}}^{(1)}} \frac{P_{\mathrm{VV}}^{(1)}/K_{\mathrm{VL}}^{(1)}}{[1 + P_{\mathrm{VV}}^{(1)}(\sigma - \sigma_{v^*})/K_{\mathrm{VL}}^{(1)}]} \frac{(2v^* - p)\Phi}{2K_{\mathrm{VL}}^{(1)}} \tag{10c}$$

As already noticed, due to the exoergic reaction the vibrational ladder is not populated according to the Boltzmann equilibrium distribution. The displacement from equilibrium, which is at the origin of the HA mechanism here discussed, is linked to the relaxation currents $I_{j,j-1}$ and, in turn, to the recombination rate. The origin of the non-equilibrium state of the adlayer is ascribed to the exothermicity of the recombination process that implies, in the proposed model, a net inward flux of vibrational quanta (energy) at steady state. In other words a part of the energy released during the reaction is used to sustain the adlayer in a non-equilibrium state, i.e. to maintain a steady overpopulation of HA.

Fig. 4 shows typical distribution functions as computed from Eq. (10). Compared to the Boltzmann distribution, also shown in the figure, the HA energy distribution adopts a "chair" form that is nearly flat for large quantum numbers. In fact, since $\gamma^{(1)} < 1$ the inequality $\gamma^{(1)n} < \Phi/(\sigma_0 K_{\mathrm{VL}}^{(1)})$ could be fulfilled for sufficiently large $n < v^*$ values; consequently the distribution becomes independent of energy and proportional to $\Phi/(\sigma_0 K_{\mathrm{VL}}^{(1)})$

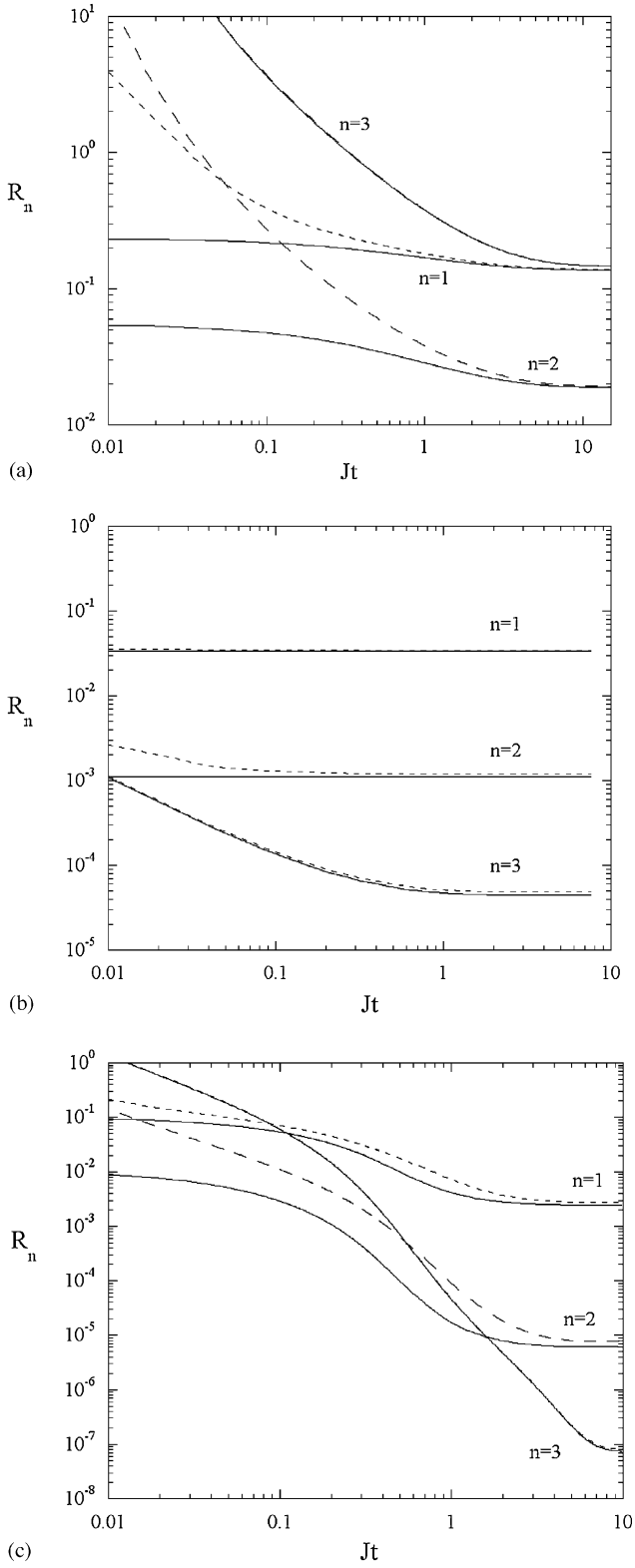

Fig. 3. Four levels system: kinetics of the populations of HA, $R_n = \sigma_n(t)/\sigma_0(t)$, for the reaction channel A. Full lines: analytical solutions which hold under quasi-steady state condition. Dashed lines: numerical solutions of the master equations. The kinetics shown in panels a, b and c have been computed for parameter values that are the same as curves a, b and c of Fig. 2, respectively.

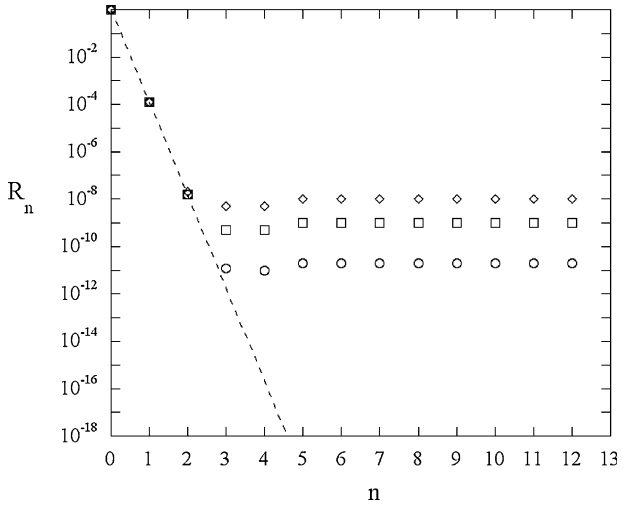

Fig. 4. Energy distribution functions for the recombination channel B. Parameter values are: $v^* = 12$, $p = 4$, $K_{VL}^{(1)} = 10^{10}\ s^{-1}$, $\beta E_{01} = 9$ and $\gamma^{(1)} \cong \gamma_B$. Circles: $\Phi/\sigma_0 = 0.2\ s^{-1}$; squares: $\Phi/\sigma_0 = 10\ s^{-1}$; diamonds: $\Phi/\sigma_0 = 100\ s^{-1}$.

(Eq. (10b)). The computations of Fig. 4 refer to the case $P_{VV}^{(1)}\sigma_0/K_{VL}^{(1)} < 1$ and $\gamma^{(1)} \cong \gamma_B$.

2.2. Kinetic transition: from thermal to hyperthermal recombination rates

The very importance of the non-equilibrium state of the adlayer in atom recombination is represented by the effect it has on the reaction rate at steady state. In order to broach this subject we evaluate the recombination rate for the reaction channel B, in the case of random adsorption of atoms and for $P_{VV}^{(1)}\sigma/K_{VL}^{(1)} \ll 1$. By using Eq. (7) the balance equation reads $2Z_{0p}\sigma\sigma_p = J(1-\sigma)$ and, by means of Eq. (10a), the normalized recombination rate, $\eta = \Phi/J$, satisfies the equation:

$$2Z'(1-\eta)\left[(1-\eta)\gamma^{(1)p} + \frac{\eta}{2K'}\right] = \eta \tag{11}$$

where Z' and K' are the rate constants normalized to J and the condition $\sigma_0 \approx \sigma = (1-\eta)$ was also employed. The behavior of η as a function of both $K_{VL}^{(1)}/2Z_{0p}$ and surface temperature is shown in Fig. 5A and B for $p = 3$, $\gamma^{(1)} = \gamma_B$ and for several values of Z'. As appears the reaction rate increases with $(K_{VL}^{(1)}/2Z_{0p})^{-1}$ and the reaction rate, compatible with the Boltzmann distribution, is practically achieved at $K_{VL}^{(1)}/Z_{0p} > 1$. On the basis of the discussion reported above, such a behavior is ascribed to a continuous transition of the vibrational state of the adlayer, which is accompanied by a large increase of both HA populations and reaction rate.

This kinetic transition has also important consequences on the amount of the adsorbed species at steady state. To illustrate this point we deal with the reaction channel B for $\sigma_p \gg \sigma\gamma_B^p$, i.e. when the surface coverage of HA is hyperthermal. In the limiting case $P_{VV}^{(1)}\sigma/K_{VL}^{(1)} \ll 1$ Eq. (10) give $\sigma_p \cong \Phi/2K_{VL}^{(1)}$ and $\sigma_{n>p} \cong \Phi/K_{VL}^{(1)}$. Therefore, at steady state the surface density of HA is constant and proportional to the reaction rate. Besides, being the reaction rate equal to $\Phi = 2Z_{0p}\sigma\sigma_p$ the inequality

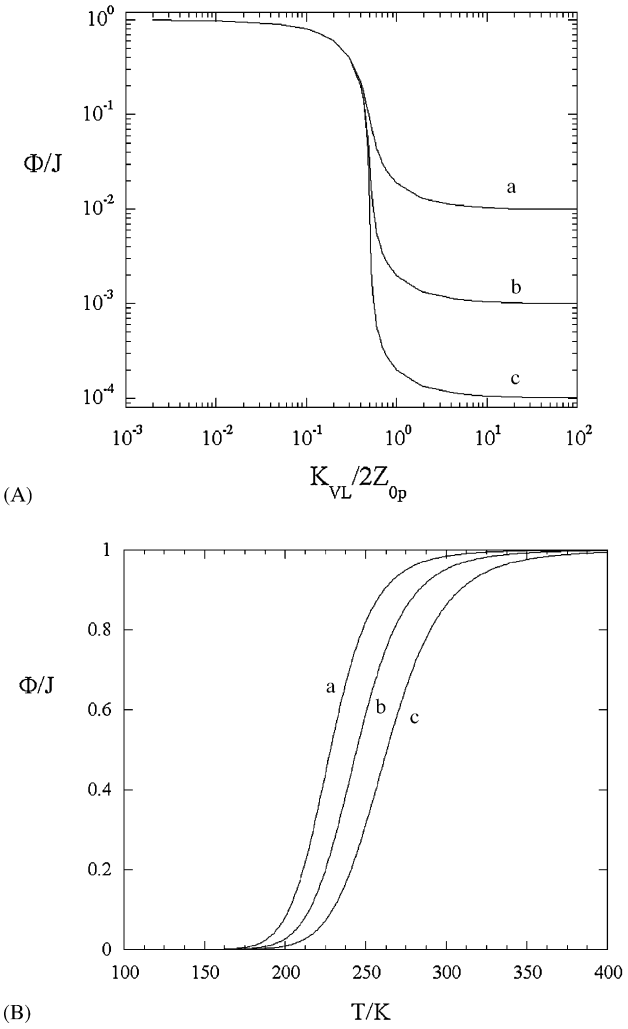

Fig. 5. Panel (A) steady state recombination rate as a function of $K_{VL}/2Z_{0p}$ for the reaction channel B at $p = 3$. Parameter values are: $\beta E_{01} = 13$, $Z_{0p} = 5 \times 10^{12}\ s^{-1}$ and $J = 0.01\ s^{-1}$ (curve a), $J = 0.1\ s^{-1}$ (curve b) and $J = 1\ s^{-1}$ (curve c). Panel (B) steady state recombination rate as a function of surface temperature, T, for the reaction channel B at $p = 3$. Parameter values are: $E_{01} = 21.6$ kJ/mol, $K_{VL}/2Z_{0p} = 0.5$ and $J = 0.01\ s^{-1}$ (curve a), $J = 0.1\ s^{-1}$ (curve b) and $J = 1\ s^{-1}$ (curve c).

$\Phi \gg \Phi_B$ is fulfilled, where $\Phi_B = 2Z_{0p}\sigma^2\gamma_B^p$ is the recombination rate in the case of Boltzmannian populations of the vibrational ladder. Under these circumstances the relationship holds $\Phi \cong 2Z_{0p}\sigma\Phi/2K_{VL}^{(1)}$, namely $\sigma \cong K_{VL}^{(1)}/Z_{0p}$. In other words, in case of hyperthermal HA energy distribution function the steady state surface coverage is equal to the ratio $K_{VL}^{(1)}/Z_{0p}$ which, in turn, ought to be lower than one. It is worth noticing that this result is independent of the functional form of the adsorption rate, $J(\sigma)$. The steady state recombination rate is equal to $J(K_{VL}^{(1)}/Z_{0p})$ and is expected to depend, weakly, on surface temperature. This is the distinctive feature of the recombination kinetics ruled by non-Boltzmannian HA energy distributions.

Let us now switch to the case $\sigma_p \cong \sigma\gamma_B^p$ which implies $\Phi \cong \Phi_B$. As a matter of fact, if the energy distribution function of the adatoms is Boltzmannian, the surface coverage should be estimated by means of the equation $J(\sigma) = 2Z_{0p}\sigma^2\gamma_B^p$, which depends on activation energy for recombination, surface temperature and $J(\sigma)$ function. Clearly, in this instance the

recombination rate is thermically activated. In the particular case of random adsorption it is given by Eq. (11), in the limit $K' \to \infty$, and turns out to be independent of relaxation time, $1/K_{VL}^{(1)}$. Conversely, for hyperthermal HA energy distribution function the recombination rate is given by $\eta \cong 1 - (K_{VL}^{(1)}/Z_{0p})$, and depends on relaxation time and recombination probability, only. The results of Fig. 5 corroborate these arguments.

2.3. The effect of multi-quantum transfer on the HA energy distribution functions

In this section we consider in more details the general case of multi-quantum transfer during adatom relaxation and its effect on the populations of HA. As already noted at steady state Eq. (4) can be iterated for any q value and this allows one to express the HA coverage as a function of the rate constants for the exchange of q quanta. For instance, in the case $q = 1$, 2 Eq. (4) leads to ($q = 2$):

$$\sigma_{2m} = \sigma_0 \gamma^{(2)^m} + \alpha^{(2)} \sum_{j=1}^{m} I_{2j,2j-2} \gamma^{(2)^{m-j}} \tag{12}$$

where $\alpha^{(2)} = [K_{VL}^{(2)} + P_{VV}^{(2)}(\sigma - \sigma_{v^*} - \sigma_{v^*-1})]^{-1}$, $\gamma^{(2)} = \gamma_B^{(2)}(1 + \xi^{(2)})$ with $\xi^{(2)} = (P_{VV}^{(2)}/\gamma_B^{(2)} K_{VL}^{(2)}) \alpha^{(2)} \sum_{j=0}^{v^*-2} I_{j+2,j}$ and $\gamma_B^{(2)} = e^{-2\beta E_{01}}$. A similar expression can be derived for odd n. It is worth noting, in passing, that $\gamma_B^{(2)}$ can be much lower than $\gamma_B^{(1)}$ and, as we will see shortly, this has important consequences on the shape of the HA energy distribution function. To further address this point we consider the reaction channel A (with p an even number) and assume that the most efficient route for energy relaxation is at $q = 2$, i.e. $K_{VL}^{(2)} \approx 1/\tau$, τ being the characteristic time for energy dissipation to the solid. Moreover, we set $I_{n,n-2} = 0$ for odd n. Since $(I_{j,j-q})_{j \le p} = 0$ by equating Eqs. (8), (12), for $n = 2m < p$, we get the following relationship between $\gamma^{(1)}$ and $\gamma^{(2)}$: $\gamma^{(1)} = \sqrt{\gamma^{(2)}}$ or

$$\xi^{(1)} = (1 + \xi^{(2)})^{1/2} - 1 \tag{13}$$

This expression indicates that $\xi^{(1)}$ can be much larger than one and this implies, to a great extent, hyperthermal energy distribution functions ($\gamma^{(1)} \gg \gamma_B$). This can be seen according to the following argument. Since the two-quantum exchange represents the main channel for energy transfer, the current $I_{j,j-2}$ is expected to be of the order of magnitude of the recombination rate (i.e. the adsorption rate) at steady state. By defining the quantity $\lambda = P_{VV}^{(2)} \sigma_0 / K_{VL}^{(2)}$ and considering that $\sigma \approx \sigma_0$, the $\xi^{(2)}$ term becomes:

$$\xi^{(2)} \approx e^{2\beta E_{01}} \frac{\lambda}{\lambda + 1} \frac{\Phi \tau}{\sigma_0} \tag{14}$$

In the case of Q quantum exchange, Eqs. (13) and (14) can be easily generalized according to:

$$\xi^{(1)} = (1 + \xi^{(Q)})^{1/Q} - 1 \tag{15a}$$

$$\xi^{(Q)} \cong e^{Q\beta E_{01}} \frac{\Phi \tau}{\sigma_0} \tag{15b}$$

which hold in the limit $\lambda > 1$. These equations show that, on account of the exponential term, the non-equilibrium factor, $\xi^{(Q)}$, can be much larger than one. As an example, assuming $Q = 3$, $\tau = 10^{-11}$ s and $\Phi = 0.5\ s^{-1}$, Eq. (15a) provides $\xi^{(1)} \approx 300$ for $T = 100$ K, $\sigma_0 = 1$ and $E_{01} = 12$ kJ/mol.

Incidentally at $n < p$ the adatom energy distribution (case A) coincides with the distribution function previously obtained by Treanor et al. [17] in the case of vibrational excitation of gas molecules. In their approach the non-equilibrium state of the system is characterized through the T_1 temperature that is linked to the population of the level $n = 1$: $\gamma^{(1)} = e^{-E_{01}/k_B T_1}$. With reference to the distribution reported in Eq. (8), we note that the first term on the right-hand side ($\gamma^{(1)n}$) actually reduces to the Treanor distribution through a suitable choice of the T_1 parameter. To be specific, the relationship between $\xi^{(1)}$ and T_1 is given by

$$\xi^{(1)} = e^{E_{01}/k_B((1/T)-(1/T_1))} - 1. \tag{16a}$$

Furthermore, by using Eq. (15) we get:

$$\frac{T}{T_1} = 1 - \frac{1}{Q\beta E_{01}} \ln\left(1 + \frac{\Phi \tau}{\sigma_0} e^{Q\beta E_{01}}\right) \tag{16b}$$

which relates the temperature T_1 to the recombination rate and characteristic time for energy relaxation. We note that Eq. (16a), which holds in the harmonic case, provides a measure of the overpopulation of the vibrational ladder (at $n < p$), when compared to the Boltzmann distribution. As a matter of fact for a Boltzmann distribution $T = T_1$; a condition that is obtained, in Eq. (16b), for $\Phi = 0$ namely in the absence of the recombination process. In other words the displacement from equilibrium, at steady state, is dictated by the reaction rate or, alternatively, by the flux of the adsorbing atoms which ''climb down'' the vibrational states of the ladder.

The argument above presented indicates that since $\xi^{(1)}$ can be much greater than one, the ''Treanor-like'' term of the distribution could be the leading one in Eq. (8). However, this is linked to the occurrence of two conditions: (i) the multi-quantum transfer and (ii) a quite efficient VV process. Under these circumstances the distribution function of the adatoms resembles the Treanor curve. It is worth noting that experimental data on deuterium abstraction by atomic hydrogen at metal surfaces have been recently used in order to obtain information on the adatom distribution functions [18]. The data analysis indicates that the vibrational populations are in reasonable accord with the Treanor distribution where the T/T_1 values depend upon the system and the experimental conditions. Besides, from the ''experimental'' T/T_1 values and Eq. (16b) it is possible to gain information on the dynamics of the relaxation process. In particular, the T/T_1 parameters as obtained for recombination at Pt, Ni and Cu surfaces are consistent with $Q = 5$ that is the exchange of five vibrational quanta per scattering event. This corresponds to an energy transfer of 0.5 eV which means about 23% of the released energy. The electron–hole (e–h) pair excitation could represent a facile relaxation route for the hot

atoms. As a matter of fact, the (e–h) pair spectrum ranges between 0 and 1.5 eV with an average energy transfer of 0.5 eV per relaxation event [19,20].

3. Conclusions

We reported on a hot atom kinetic model for describing diatom recombination at catalytic surfaces. Hot atoms are identified with the adatoms in the excited vibrational states. The populations of HA under steady state conditions have been computed in closed form. The overpopulation of the upper bound level is dictated by the ratio between adsorption flux and rate constant for VL dissipation and can be larger than one by order of magnitudes. This implies a strong coupling between adsorption and desorption processes as experimentally observed in the ASD. The overpopulation of the vibrational ladder also affects the rate of diatom recombination; in this respect the computation indicates the occurrence of transitions – from equilibrium to non-equilibrium states – which are characterized by an increase of the reaction rate. The most significant control parameter is found to be the ratio between the probabilities for diatom formation and for energy transfer to the solid.

The effect of multi-quantum transfer on the vibrational distribution functions has also been analysed. The computation shows that the distribution derived by Treanor et al. can be achieved at steady state provided the VV process is efficient. The temperature $T_1 > T$, which determines the overpopulation of the first vibrational level, has been determined as a function of the number of vibrational quanta transferred to the solid. Application of the model to experimental data on H recombination at metal surfaces gives a value of five quanta per relaxation event that is compatible with an e–h pair excitation.

Appendix A

In this appendix we derive Eq. (8) that holds in the harmonic case and for $q = 1$. To begin with we rewrite Eq. (4) according to:

$$\sigma_n = \gamma_n^{(1)}\sigma_{n-1} + \alpha_n^{(1)} I_{n,n-1}. \tag{A.1}$$

where

$$\gamma_n^{(1)} = \left(\frac{K_{-(n-1)}^{(1)}}{K_n^{(1)}} + \frac{P_{(n-1)}^{f(1)}}{K_n^{(1)}}\right)\left(1 + \frac{P_n^{r(1)}}{K_n^{(1)}}\right)^{-1} \tag{A.2}$$

and

$$\alpha_n^{(1)} = (K_n^{(1)} + P_n^{r(1)})^{-1}. \tag{A.3}$$

By making use of the detailed balancing ($P_{n-1,s\to n,s-1}^{(1)} = P_{n,s-1\to n-1,s}^{(1)}$) in Eq. (5), one obtains:

$$P_{n-1}^{f(1)} = \sum_{s=1}^{v^*} P_{n,s-1\to n-1,s}\sigma_s = \sum_{j=0}^{v^*-1} P_{n,j\to n-1,j+1}\sigma_{j+1} \tag{A.4}$$

Also, application of the detailed balance to the VL scattering leads to:

$$\frac{K_{-(n-1)}^{(1)}}{K_n^{(1)}} = \mathrm{e}^{-\beta E_{01}} \equiv \gamma_{\mathrm{B}}^{(1)}. \tag{A.5}$$

In the case of rate constants independent of quantum numbers, i.e. $P_{n,s\to n-1,s+1} \equiv P_{\mathrm{VV}}^{(1)}$ and $K_n^{(1)} \equiv K_{\mathrm{VL}}^{(1)}$, Eqs. (A.2) and (A.3), become:

$$\gamma^{(1)} = \left(\gamma_{\mathrm{B}}^{(1)} + \frac{P_{\mathrm{VV}}^{(1)}}{K_{\mathrm{VL}}^{(1)}}\sum_{s=0}^{v^*-1}\sigma_{s+1}\right)\left(1 + \frac{P_{\mathrm{VV}}^{(1)}}{K_{\mathrm{VL}}^{(1)}}\sum_{s=0}^{v^*-1}\sigma_s\right)^{-1} \tag{A.6}$$

$$\alpha^{(1)} = \left(K_{\mathrm{VL}}^{(1)} + P_{\mathrm{VV}}^{(1)}\sum_{s=0}^{v^*-1}\sigma_s\right)^{-1} = (K_{\mathrm{VL}}^{(1)} + P_{\mathrm{VV}}^{(1)}(\sigma - \sigma_{v^*}))^{-1} \tag{A.7}$$

where use has been made of Eqs. (6), (A.4) and (A.5). By substituting Eq. (A.1) in expression (A.6) we get:

$$\gamma^{(1)} = \gamma_{\mathrm{B}}^{(1)} + \frac{P_{\mathrm{VV}}^{(1)}}{K_{\mathrm{VL}}^{(1)}}\sum_{s=0}^{v^*-1}(\sigma_{s+1} - \gamma^{(1)}\sigma_s) \tag{A.8}$$

which, once simplified by means of Eq. (A.1), provides the result reported in Section 2.1:

$$\gamma^{(1)} = \gamma_{\mathrm{B}}^{(1)} + \frac{P_{\mathrm{VV}}^{(1)}\alpha^{(1)}}{K_{\mathrm{VL}}^{(1)}}\sum_{s=0}^{v^*-1} I_{s+1,s}\,.$$

Let us now consider the evaluation of σ_n. We limit the demonstration to the case $n \leq 3$. Eq. (A.1) reads:

$$\sigma_1 = \sigma_0\gamma^{(1)} + \alpha^{(1)} I_{1,0} \tag{A.9}$$

$$\sigma_2 = \sigma_1\gamma^{(1)} + \alpha^{(1)} I_{2,1} \tag{A.10}$$

$$\sigma_3 = \sigma_2\gamma^{(1)} + \alpha^{(1)} I_{3,2}\,. \tag{A.11}$$

By inserting Eq. (A.9) in Eq. (A.10) and Eq. (A.10) in Eq. (A.11) we end up with

$$\begin{aligned}\sigma_2 &= (\sigma_0\gamma^{(1)} + \alpha^{(1)} I_{1,0})\gamma^{(1)} + \alpha^{(1)} I_{2,1} \\ &= \sigma_0(\gamma^{(1)})^2 + \alpha^{(1)}\sum_{j=1}^{2} I_{j,j-1}(\gamma^{(1)})^{2-j}\end{aligned} \tag{A.12}$$

$$\begin{aligned}\sigma_3 &= \sigma_0(\gamma^{(1)})^3 + \alpha^{(1)} I_{1,0}(\gamma^{(1)})^2 + \alpha^{(1)} I_{2,1}(\gamma^{(1)}) + \alpha^{(1)} I_{3,2} \\ &= \sigma_0(\gamma^{(1)})^3 + \alpha^{(1)}\sum_{j=1}^{3} I_{j,j-1}(\gamma^{(1)})^{3-j}\end{aligned} \tag{A.13}$$

that is Eq. (8) for $n = 3$.

References

[1] L. Romm, M. Asscher, Y. Zeiri, J. Chem. Phys. 110 (1999) 11023.
[2] J.C. Tully, Ann. Rev. Phys. Chem. 51 (2000) 153.
[3] V.P. Zhdanov, K.I. Zamaraev, Catal. Rev. Sci. Eng. 24 (3) (1982) 373.
[4] T.A. Jachimowski, W.H. Weinberg, J. Chem. Phys. 101 (1994) 10997.

[5] J. Harris, B. Kasemo, Surf. Sci. 105 (1981) L281.
[6] Th. Kammler, D. Kolovos-Vellianitis, J. Küppers, Surf. Sci. 460 (2000) 91.
[7] B. Jackson, X. Sha, Z.B. Guvenc, J. Chem. Phys. 116 (2002) 2599.
[8] J.Y. Kim, J. Lee, J. Chem. Phys. 113 (2000) 2856.
[9] D. Kolovos-Vellianitis, J. Küppers, Surf. Sci. 584 (2004) 67.
[10] E. Molinari, M. Tomellini, Chem. Phys. 270 (2001) 439.
[11] S. Whener, J. Küppers, J. Chem. Phys. 108 (1998) 3353.
[12] C. Wei, G.L. Haller, J. Chem. Phys. 105 (1996) 810.
[13] E. Molinari, M. Tomellini, Chem. Phys. 277 (2002) 373.
[14] M. Tomellini, Surf. Sci. 577 (2005) 200.
[15] E. Molinari, M. Tomellini, Surf. Sci. 552 (2004) 180.
[16] M. Tomellini, Surf. Sci. 556 (2/3) (2004) 184.
[17] C. Treanor, J.W. Rich, R.G. Rehm, J. Chem. Phys. 48 (1968) 1798.
[18] E. Molinari, M. Tomellini, Surf. Sci. 600 (2) (2006) 273.
[19] H. Nienhaus, Surf. Sci. Rep. 45 (2002) 1.
[20] K. Schönhammer, O. Gunnarsson, Phys. Rev. B 22 (1980) 1629.